

# Impacts of Fluorine and Nitrogen Incorporation on NiSi Induced Junction Leakage on Si(110) Substrate

Masakatsu Tsuchiaki and Akira Nishiyama

Corporate Research & Development Center, Toshiba Corporation.

c/o 8 Shinsugita-cho, Isogo-ku, Yokohama, 235-8522, Japan

Phone:+81-45-770-3229 Fax:+81-45-770-3286 E-mail:masakatsu.tsuchiaki@toshiba.co.jp

## 1. Introduction

For sheet resistance reduction of ever shallowing S/D junctions, NiSi is now utilized as a primary SALICIDE material due to its small Si consumption and low formation temperature [1]. At the same time, in an effort to maximize the current drivability, growing attention is now directed toward CMOS integration over a hybrid orientation substrate, forming nFETs and pFETs on Si(100) and Si(110) surfaces, respectively [2]. Recently, however, an in-depth study of thin NiSi films formed on both surfaces has revealed thermal instability and associated substantial leakage generation on shallow junctions even during thermal processing at 500°C (i.e., a typical temperature for interlayer formation by CVD)[3]. Since such low temperature intolerance significantly impairs device manufacturability, a way must be devised to stabilize NiSi films against heat stimulus. One of the most practical and convenient means of such thermal stabilization would be pre-SALICIDE ion implantation (PSII) prior to the silicidation. In fact, regarding NiSi on Si(100), drastic leakage suppression by F-PSII has been demonstrated lately [4]. Nevertheless, with respect to reduction of the thermally induced leakage of NiSi on Si(110), a sensitive and comparative investigation on PSII's efficiency and influence of the crystal orientation has never been conducted. Hence, we herewith report on a basic and systematic study of PSII's effects on NiSi on Si(110), in full contrast with Si(100). Impacts of light non-dopant ions (i.e., F and N) are thoroughly examined. For the first time, crystal orientation dependency of PSII's effects is evidenced and its physical and practical implication is discussed.

## 2. Junction Formation and PSII

Fig.1 illustrates the procedure for junction formation allowing a sensitive study. The details of the fabrication will be found in ref. [5]. After formation of a virtually flat p-well over 8-inch, p-type, CZ, Si(100) or Si(110) wafers, a junction region is delineated by RIE-etching a SiN film and wet-etching an underlying TEOS film, avoiding plasma damage to the substrate (Fig.1-a). Subsequently, in order to facilitate fair and clear comparison, on both Si(100) and Si(110) substrates, AsSG film is deposited and annealed to form an n+ region by solid phase diffusion into the opening defined above (Fig.1-b). By adjusting the annealing time and temperature, n+/p junctions with various depths,  $x_j$  can be readily obtained [5]. After AsSG removal by wet etching, SiN sidewalls are formed to guard the periphery (Fig.1-c). Then, to assess PSII's effects, F and N are implanted. The dose,  $\Phi$ , is varied up to  $1 \times 10^{15} \text{cm}^{-2}$ . The energy is set to be 2keV, so that the projection ranges (about 10nm) are contained within the silicide layers to be formed. Because F and N have similar atomic weights, this experiment can also contrast chemical difference due to PSII ions, while maintaining almost identical physical damage. Finally, a silicidation process is applied, forming about 30-nm-thick NiSi film to complete the junction structure (Fig.1-d).

## 3. Leakage Suppression: F-PSII vs. N-PSII

In order to assess impacts of thermal processing on junction leakage, the above junctions are annealed in  $\text{N}_2$  at 500 °C for 90min. Then, effects of PSII on leakage are monitored for various  $\Phi$  and  $x_j$ . In Fig.2 and Fig.3, leakage depths (i.e., depth at  $I_R=10^{-6} \text{A/cm}^2$ ) are plotted as functions of  $\Phi$  for Si(100) and Si(110), respectively. Evidently, on Si(100), shallower junctions are attainable with F-PSII. On Si(110), however, N-PSII's efficiency improves substantially, even surpassing F-PSII at  $\Phi = 1 \times 10^{14} \text{cm}^{-2}$ . In Fig.4 and Fig.5, leakage levels at this dosage are respectively plotted as functions of the junction depth (right axes) and correlated with Ni backside SIMS profiles (left axes). The excellent matching between the leakage-depth profiles and Ni

SIMS data clearly proves leakage suppression by hindering Ni ingress into the Si substrates, regardless of their orientation. However, specific to Si(110) is the presence of long tails in the leakage-depth profiles. Corresponding channeling tails in SIMS profiles of F and N (Figs.6 and 7) are distinctly present only in Si(110), revealing PSII as a cause of the excess leakage generation. In order to remove this undesirable PSII damage and also to probe impacts of S/D activation on PSII, RTA (1000°C, 10s) is tried between PSII ( $\Phi = 1 \times 10^{15} \text{cm}^{-2}$ ) and silicidation. As shown in Figs.8 and 9, by RTA, both PSII ions out-diffuse rapidly and only those trapped at defects around the projection range are incorporated within the NiSi. Strikingly, however, this in-film confinement has significant impacts on the leakage. As evident on Si(100) (Fig.10), in-film F has no ability to reduce leakage, although enough in-film F (comparable to interfacial F at  $\Phi = 1 \times 10^{14} \text{cm}^{-2}$ , Fig.6) is present. Since F-PSII works well without extensive F's presence in the substrate (Figs.4 and 6), the leakage suppression by F-PSII is achieved predominantly by interfacial F and halfway suppression in Fig.11 is likely due to the small F's pile-up at the interface (Fig.9). In contrast, as evident on Si(110) (Figs.9 and 11), in-film N seems to retain matching efficiency for that of RTA-less N-PSII with a corresponding amount of N incorporation ( $\Phi = 1 \times 10^{13} \text{cm}^{-2}$ ). Moreover, similar leakage suppression is achieved even by about an order of smaller N incorporation than that of F. Clearly, PSII's leakage suppression is mainly due to F's passivation of the NiSi/Si interface or N's stabilization of the NiSi layer (Fig.12). Particularly, F's interfacial passivation becomes indispensable for randomly oriented NiSi on Si(100) (Fig.13), because, among various configurations, the least stable interface (which is the primary source of Ni's burst into Si(100)) must be protected firmly. On the other hand, N's in-film stabilization becomes efficient for highly oriented NiSi on Si(110) (Fig.13). This is probably because highly oriented NiSi/Si(110) interface is relatively stable and Ni burst is more originated inside NiSi, possibly at grain boundaries, than at the interface. Although N's presence at the grain boundaries may have caused sheet resistance increase at a high dose (Fig.14), N incorporation (at least up to  $\Phi = 5 \times 10^{14} \text{cm}^{-2}$ ) provides a useful and complementary way of leakage suppression on Si(110), without any disturbance in contact resistance (Fig.15). Especially, leakage suppression by in-film N will allow large latitude in the way of damage-free N incorporation, such as N doping during S/D elevation or during Ni sputtering [6], whereas introduction of interfacial F practically requires implantation just prior to the silicidation. Considering Si(110)'s vulnerability to the light ion channeling (which may not be completely avoided even by tilted implantation), the best way of leakage suppression on a hybrid orientation substrate would be a low dose or selective F-PSII just prior to the silicidation for Si(100), complemented by damage-free N doping or high dose N-PSII together with S/D implantation for Si(110).

## 4. Summary and Conclusion

Effects of F and N on NiSi on Si(110), are thoroughly examined in full contrast with Si(100). Unlike Si(100), it is found that low dose N-PSII can suppress leakage quite efficiently on Si(110), by stabilizing grain boundaries of highly oriented NiSi on Si(110). Damage-free N doping will provide a useful way of leakage suppression on Si(110), without undesirable channeling damage inherent to this orientation.

## References

- [1] T. Morimoto et al., IEEE Trans. E.D., 42, 915 (1995)
- [2] C.Y.Sung et al, IEDM Tech. Dig., 2005, p.235
- [3] M. Tsuchiaki et al., Ext. Abs. SSDM., 2006, p.340
- [4] M. Tsuchiaki et al., Jpn. J. Appl. Phys., 44, 1673 (2005)
- [5] M. Tsuchiaki et al., Jpn. J. Appl. Phys., 43, 5166 (2004)
- [6] T.Ohguero et al., IEDM Tech. Dig., 1995, p.453

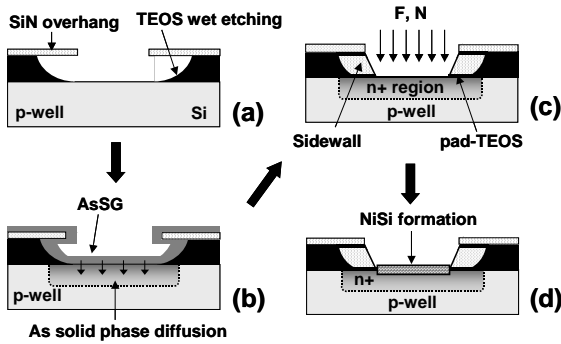


**Fig.1** n+/p junction formation procedure to fabricate damage-free diodes. (a) Isolation is achieved by wet etching of TEOS. (b) Solid phase diffusion from AsSG is used for creating n+ region. (c) Sidewall is formed and PSII with F and N is applied. (d) NiSi is formed.

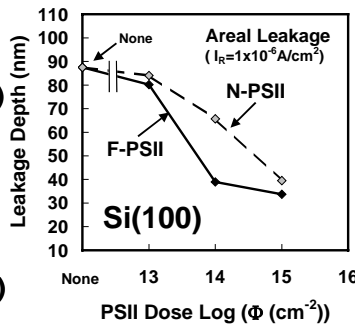


**Fig.2** Leakage depths (i.e., minimum junction depth from NiSi bottom to keep leakage less than  $I_R=1 \times 10^{-6} \text{ A/cm}^2$ ) plotted as functions of PSII dose  $\Phi$  on Si(100). F-PSII is much more efficient than N-PSII.

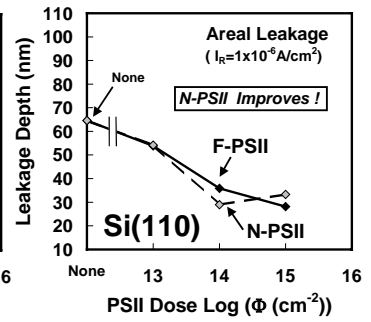


**Fig.3** Leakage depths plotted as functions of PSII dose on Si(110). Unlike Si(100), N-PSII becomes more efficient than F-PSII at  $\Phi=1 \times 10^{14} \text{ cm}^{-2}$ , revealing crystal orientation dependency of PSII's effects.

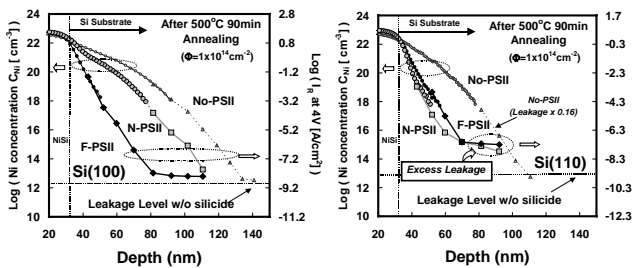


**Fig.4** Comparison between Ni SIMS profiles and leakage-depth profiles of F-PSII and N-PSII on Si(100) after 500°C, 90min annealing. For reference, profile of no-PSII sample is included.

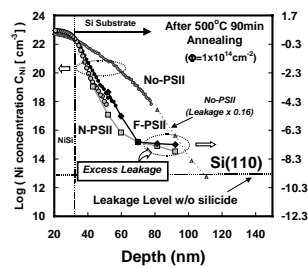


**Fig.5** Comparison between Ni SIMS profiles and leakage-depth profiles of F-PSII and N-PSII on Si(110) after 500°C, 90min annealing. Presence of long tails are evident.

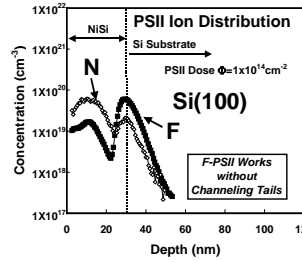


**Fig.6** Depth profiles of F and N after NiSi formation on Si(100). Although N is incorporated mainly in the NiSi film, substantial F remains around NiSi/Ni interface.

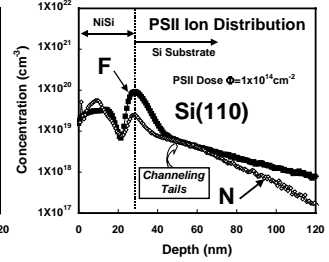


**Fig.7** Depth profiles of F and N after NiSi formation on Si(110). Presence of channeling tails are conspicuous for both F and N

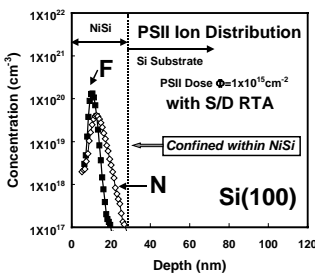


**Fig.8** Depth profiles of F and N after S/D activation RTA and NiSi formation on Si(100). Both F and N are entirely incorporated within the NiSi film. PSII ions out-diffuse during S/D RTA except around projection ranges.

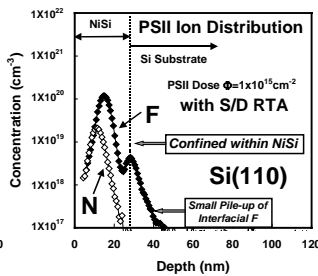


**Fig.9** Depth profiles of F and N after S/D activation RTA and NiSi formation on Si(110). While N is incorporated entirely within the NiSi film, a small amount of F piles up at the interface.

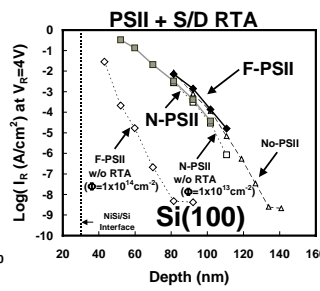


**Fig.10** Leakage levels of RTA-treated PSII samples on Si(100) substrates plotted as functions of junction depth after 500°C, 90min annealing. For reference, profiles of no-PSII and RTA-free PSII samples with corresponding amounts of ion incorporation are also included.

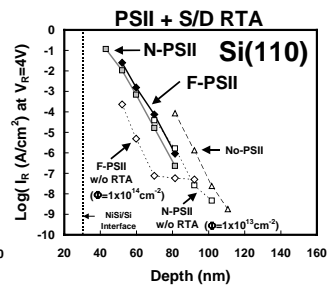


**Fig.11** Leakage levels of RTA-treated PSII samples on Si(110) substrates plotted as functions of junction depth after 500°C, 90min annealing. For reference, profiles of no-PSII and RTA-free PSII samples with corresponding amounts of ion incorporation are also included.

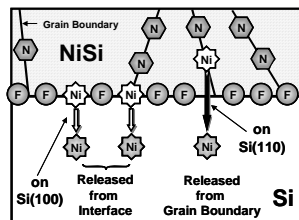


**Fig.12** Schematic diagram explaining principal mechanisms of NiSi thermal stabilization by PSII ions. F passivates NiSi/Si interface, whereas N mainly stabilizes NiSi layer at grain boundaries. The different mechanisms are responsible for the crystal orientation dependency of PSII's leakage suppression efficiency

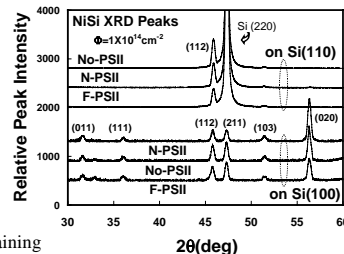


**Fig.13**  $\theta/2\theta$  XRD spectra for various PSII conditions for both Si substrates. Regardless of PSII conditions, NiSi is randomly aligned on Si(100), whereas NiSi is highly oriented on Si(110).

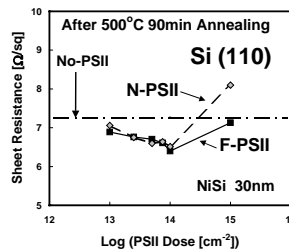


**Fig.14** Sheet resistance of 30nm NiSi plotted as a function of PSII dose on Si(110). An increase for high dose N-PSII could be caused by N's preferential incorporation at grain boundaries

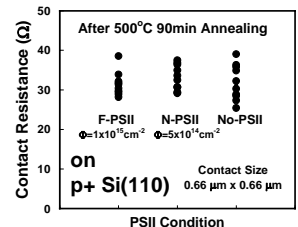


**Fig.15** Contact resistance of NiSi to p+Si(110). Irrespective of F-PSII with  $\Phi=1 \times 10^{15} \text{ cm}^{-2}$  and N-PSII with  $\Phi=5 \times 10^{14} \text{ cm}^{-2}$ , contact resistance stays intact.